

Synthesis and Surface Properties of Novel Quaternary Ammonium Gemini Surfactants with Polar Head Groups Containing 2-Hydroxypropyl Moieties

Yun Bai¹ · Chunsheng Pu¹  · Shuai Liu¹ · Xiang Gao¹ · Gang Chen²

Received: 5 August 2020 / Revised: 18 January 2021 / Accepted: 18 January 2021
© 2021 AOCS

Abstract The purpose of this paper is to comprehend in-depth the effect of the surfactant structure on its and physicochemical properties such as surface/interfacial properties, foam stability, wettability, and biodegradability. To this end, quaternary ammonium Gemini surfactants, alkanediyl- α,ω -bis[(2-hydroxypropyl)dodecylammonium] dibromide (abbreviated as C_m -n- C_m [iso-Pr(OH)]₂ with $m = 12, 14$ and $n = 2, 3, 4$) were synthesized *via* substitution and quaternization reactions, and their chemical structures were characterized by Fourier transform infrared (FT-IR) and nuclear magnetic resonance (¹HNMR) spectroscopies. The results showed that with the decrease of the spacer length, the surface tension was reduced more strongly, and with the increase of the alkyl tail length, micelles were more easily formed. Besides, the highest surface activity of C_{14} -2- C_{14} [iso-Pr(OH)]₂ was observed by increasing NaCl concentration to 200 g L⁻¹. The temperature had a great influence on thermodynamic parameters of the adsorption and micellization. The interfacial tension between 0.26 g L⁻¹ C_{14} -2- C_{14} [iso-Pr(OH)]₂ solution and oil could reach 0.022 mN m⁻¹. An elongation of the spacer chain in C_{14} -n- C_{14} [iso-Pr(OH)]₂ was unfavorable to foam stability.

Besides, the oil-wetted core, which was aged in 0.6 g L⁻¹ C_{14} -2- C_{14} [iso-Pr(OH)]₂ solution, exhibited more hydrophobicity. C_m -n- C_m [iso-Pr(OH)]₂ surfactants produced higher biodegradable rates in river water ($\geq 90\%$ after 28 days) than the biodegradable surfactant of international recommendation (71% after 28 days) at 30 °C.

Keywords Gemini cationic surfactants · Surface/interfacial properties · Foam stability · Wettability · Biodegradability

J Surfact Deterg (2021) 24: 199–208.

Introduction

Surfactants are indispensable auxiliary agents that have many applications in textile, pharmaceutical, petroleum, food, and other industries (Hao et al., 2019). One class of surfactants is Gemini surfactants, which are composed of two hydrophobic chains and two polar head groups linked together by the spacer (Sharma et al., 2017). These surfactants were first reported by Bunton et al. (1971) and then named “Gemini” by Menger and Littau (1991). Subsequent studies found that Gemini surfactants were superior to single-chain surfactants in terms of interfacial activities, wettability, and antibacterial activity (Hegazy et al., 2015). Gemini surfactants are classified into different types according to the nature of head groups. The most studied cationic Gemini surfactants are quaternary ammonium-based due to their ability to adsorb to the solid surface with negative charges, so they are used as the flotation agents, antistatic agents, buffers, and emulsifiers (Kaur et al., 2013). To broaden their application range, new

Supporting information Additional supporting information may be found online in the Supporting Information section at the end of the article.

✉ Chunsheng Pu
chshpu_tx@126.com

¹ School of Petroleum Engineering, China University of Petroleum, Qingdao, 266580, China

² Shaanxi Province Key Laboratory of Environmental Pollution Control and Reservoir Protection Technology of Oilfields, Xi’an Shiyou University, Xi’an, 710065, China

functional groups such as hydroxyl, amide, and ester, have been introduced into head groups of quaternary ammonium Gemini surfactants (Wu et al., 2020).

It has been reported in the literature that Gemini surfactants with head groups possessing hydroxymethyl moieties have better physicochemical properties than Gemini surfactants with head groups containing methyl groups due to the ability of hydroxymethyl moieties to hydrogen bond with water molecules (Teresa et al., 2016). The presence of hydrogen bond can reduce the electrostatic repulsions between positively charged head groups, so that surfactant molecules are arranged tightly on the water-air interface, thereby improving surface activity (Wang et al., 2019). The interaction between hydrogen bond increases and in turn, the strength of the liquid film enhances, making it difficult for the liquid in foams to flow from one bubble to another, which is conducive to stabilize foam. The study by Wang et al. (2019) investigated the properties of Gemini surfactants with head groups containing hydroxymethyl moieties. In this study, alkanediyl- α,ω -bis[(2-hydroxypropyl)dodecylammonium] dibromide (abbreviated as C_m - n - C_m [iso-Pr(OH)]₂ with $m = 12, 14$ and $n = 2, 3, 4$) were synthesized *via* substitution and quaternization reactions.

Quaternary ammonium Gemini surfactants, especially conventional alkanediyl - α, ω -bis (dialkylammonium bromide) are abbreviated using m - n - m with m and n representing the length of the alkyl tail and spacer, respectively. For these surfactants, the variation of their properties depends on the alkyl tail and spacer (Wen et al., 2020). Generally speaking, the influence of the alkyl tail on the surface activity of Gemini surfactants is similar to that of single-chain surfactants, while the effect of the spacer on the surface activity of Gemini surfactants is more complicated. Mathias et al. (2001) reported that the surface tension was lower for Gemini surfactants with flexible spacers than Gemini surfactants with rigid spacers. Alami et al. (1993) showed Gemini surfactant containing the spacer with less than three carbon atoms tended to form wormlike micelles in the aqueous solution without inorganic salts or hydrophobic counterions. However, for a long spacer over 13 carbon atoms, Gemini surfactants easily formed vesicles.

Most previous studies focused on evaluating simply the surface activity of surfactant dispersed in distilled water at room temperature (25 °C), while only a few studies analyzed in detail the absorption and aggregation behavior of surfactant in the presence of high salinity and temperature. Furthermore, the influence of the alkyl tail and spacer lengths on foam stability and wettability have not been reported. To this end, quaternary ammonium Gemini surfactants, alkanediyl- α,ω -bis[(2-hydroxypropyl)dodecylammonium] dibromide (abbreviated as C_m - n - C_m [iso-Pr(OH)]₂ with $m = 12, 14$ and $n = 2, 3, 4$) were synthesized, and their structures were characterized by Fourier transform infrared (FT-IR) and nuclear

magnetic resonance (¹HNMR) spectroscopies. Then, the surface/interfacial properties, foam stability, wettability, biodegradability were evaluated. This study is of great significance in helping to comprehensively understand the structure-property relationship of Gemini surfactants.

Materials and Methods

Materials

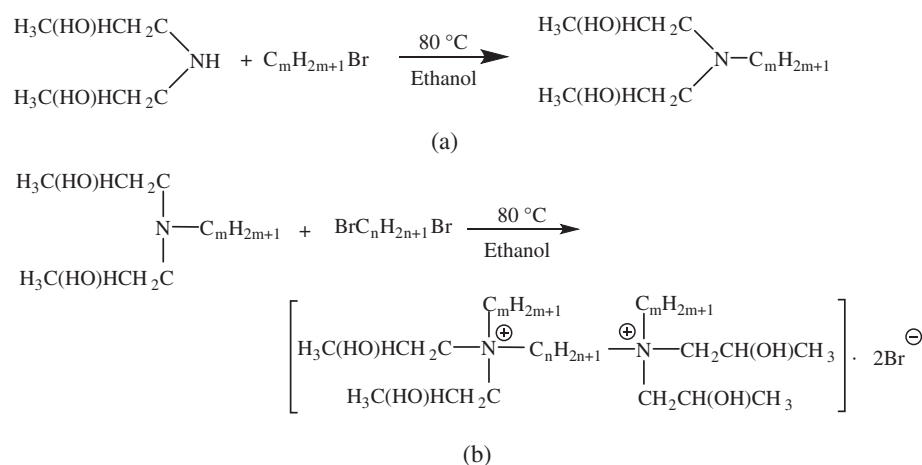
The needed reagents with purity higher than 99% such as 1-bromotetradecane, 1-bromododecane, diisopropylamine, 1,2-dibromoethane, 1,3-dibromopropane, 1,4-dibromobutane, ethyl acetate, ethanol, acetone, toluene, heptane, and sodium chloride, were obtained from Kelong Industry (Chengdu, China). Kerosene was purchased from Aladdin Chemical Reagents Company (Shanghai, China). The sandstone core plug and crude oil were collected from Chang 6 formation located in Yanchang oilfield (Yanan, China). The basic properties of crude oil were listed in the Table S1. The oil used in this study was made by 1:3 vol ratio of crude oil and kerosene, and its viscosity was 5.23 mPa·s at 30 °C. The viscosity of crude oil and kerosene at 30 °C was 20.85 and 3.32 mPa·s, respectively.

Methods

Syntheses of C_m - n - C_m [iso-Pr(OH)]₂ Surfactants

To achieve the substitution reaction (Scheme 1a), samples of (0.12 mol) 29.88 g of 1-bromododecane and (0.10 mol) 10.10 g of diisopropylamine were refluxed with (4.35 mol) 200 mL of ethanol at 80 °C for 12 h. After the completion of the reaction, a white, paste-like substance was collected by removing ethanol, and then washed with acetone three times. *N,N'*-bis(2-hydroxypropyl) dodecylamine was obtained and its yield was approximately 90.02%. To prepare *N,N'*-bis(2-hydroxypropyl) tetradecylamine, (0.12 mol) 33.24 g of 1-bromotetradecane, and (0.10 mol) 10.10 g of diisopropylamine in (4.35 mol) 200 mL of ethanol were reacted according to the method described above. The yield of *N,N'*-bis(2-hydroxypropyl) tetradecylamine was approximately 87.05%.

To achieve the quaternization reaction (Scheme 1b), samples of (0.21 mol) 69.09 g of *N,N'*-bis(2-hydroxypropyl) tetradecylamine and (0.10 mol) 18.70 g of 1,2-dibromoethane (or respective amount of 1,3-dibromopropane and 1,4-dibromobutane) were refluxed with (4.35 mol) 200 mL of ethanol at 80 °C for 24 h. After the completion of the reaction, the three yellow substances were collected by removing ethanol, then washed with acetone three times and



Scheme 1 Scheme of substitution reaction (a) and quaternization reaction (b) for $\text{C}_m\text{-n-C}_m[\text{iso-Pr}(\text{OH})]_2$ surfactants

finally, recrystallized with (0.10 mol) 10 mL of ethyl acetate and (3.43 mol) 200 mL of ethanol three times. 1-2-tetramethylene-bis[(2-hydroxypropyl)tetradecylammonium] dibromide ($\text{C}_{14}\text{-2-C}_{14}[\text{iso-Pr}(\text{OH})]_2$), 1,3-dibromopropane-bis[(2-hydroxypropyl)tetradecylammonium] dibromide ($\text{C}_{14}\text{-3-C}_{14}[\text{iso-Pr}(\text{OH})]_2$), and 1,4-dibromobutane-bis[(2-hydroxypropyl)tetradecylammonium] dibromide ($\text{C}_{14}\text{-4-C}_{14}[\text{iso-Pr}(\text{OH})]_2$) were obtained and their yields were approximately 21.54%, 22.72%, and 24.02%, respectively. To prepare 1,3-dibromopropane-bis[(2-hydroxypropyl)dodecylammonium] dibromide ($\text{C}_{12}\text{-3-C}_{12}[\text{iso-Pr}(\text{OH})]_2$), (0.21 mol) 63.21 g of *N,N'*-bis(2-hydroxypropyl) dodecylamine, and (0.10 mol) 20.10 g of 1,3-dibromopropane in (4.35 mol) 200 mL of ethanol were reacted according to the method described above. The yield of $\text{C}_{12}\text{-3-C}_{12}[\text{iso-Pr}(\text{OH})]_2$ was approximately 25.05%.

Surfactant Solution Preparation

A selected amount of surfactant was weighed and then dispersed in sodium chloride (NaCl) solution of various salinities. Subsequently, the surfactant solution was transferred to a 100 mL volumetric flask, then shaken up and down. After the completion of these steps, the surfactant volume was retained at 100 mL. To obtain the required surfactant concentration for specific experiments, the surfactant stock solution underwent dilution.

Measurements

Surface Tension

The surface tension measurement was conducted to use a surface tensiometer (DCAT 25, Aurdano Instruments Co., Ltd, Beijing, China) by the platinum ring method. Each

experiment was repeated at least three times to ensure reproducibility of results.

Interfacial Tension

A rotating interfacial tensiometer (TX-500C, Zhongchen Digital Technology Co., Ltd, Shanghai, China) was employed to measure the interfacial tension between the oil and surfactant solutions. The rotation rate was fixed at 6000 rpm. Each experiment was repeated at least three times to ensure reproducibility of results.

Foam Stability

Surfactant solution (100 mL) was blended at 7000 rpm for 3 min by using Waring Blender (Haitong da Special Instrument Co., Ltd, Qingdao, China), foams were then poured into a measuring cylinder. The half-life (a time required for the initial foam volume to be reduced by 50%) represented foam stability. Each measurement was repeated at least three times to ensure reproducibility of results.

Contact Angle

To explore the potential ability of surfactants to alter wettability in oil-wet sandstone cores, firstly, the sandstone core plug was cut into the cores with a radius of 12.0 mm and a height of 2.5 mm using a trimming machine. Following that, the cores were aged in the oil at 60 °C and atmospheric pressure. After 1 week, the cores were taken out, washed quickly with toluene and heptane (2:1 volumetric ratio) to remove the oil on the surface of the cores, and then dried in a desiccator for 12 h. After the completion of these steps, the oil-wet cores obtained were put in a transparent container containing surfactant solutions at 60 °C. After

2 weeks, 5 μL of oil droplet was released from the bottom of the container and adhered to cores. Finally, a series of images were captured by a contact angle meter (XG-CAMD, Sunzern Instruments Co., Ltd, China) and the water-phase contact angle values of images were measured using the DinoCapture 2.0 software. Each measurement was repeated at least three times to ensure reproducibility of results.

Biodegradability

The biodegradability of surfactants in river water was determined by the surface tension method using a DCAT 25 surface tensiometer (Tawfik, 2015). In this method, each surfactant was dispersed in river water at the critical micellization concentration (CMC) and incubated at 30 °C. A sample was withdrawn daily (for 28 days), filtered, and the surface tension was measured. Each measurement was repeated at least three times to ensure reproducibility of results. The biodegradation percent (D %) was calculated as follows:

$$D\% = \frac{\gamma_t - \gamma_0}{\gamma_{br} - \gamma_0} \times 100 \quad (1)$$

where γ_t is the surface tension at time t , γ_0 is the surface tension at time = 0 (initial surface tension) and γ_{br} is the surface tension of river water without the addition of surfactants at time t .

Results and Discussion

Synthesis of $C_m\text{-}n\text{-}C_m[\text{iso-Pr}(\text{OH})_2]$ Surfactants

To synthesize $C_m\text{-}n\text{-}C_m[\text{iso-Pr}(\text{OH})_2]$ surfactants, a two-step reaction was conducted (Scheme 1). In the first step, for using brominated alkanes and diisopropylamine as reactants, N,N' -bis(2-hydroxypropyl) dodecylamine and N,N' -bis(2-hydroxypropyl) tetradecylamine are obtained *via* a substitution reaction. The reaction mechanism is explained as follows: In brominated alkanes, the electronegativity of the bromine atom is greater than that of the carbon atom. The electron cloud density of the C-Br bond is higher near the bromine atom, which renders the bromine atom partially negatively charged and the carbon atom partially positively charged. Therefore, the carbon atom bound to the bromine atom is easily attacked by nitrogen in alcohol amine.

In the second step, the intermediate products, N,N' -bis(2-hydroxypropyl) dodecylamine and N,N' -bis(2-hydroxypropyl) tetradecylamine, are converted to quaternary ammonium salts *via* a quaternization reaction with dibromoalkanes. The nitrogen atoms in intermediate products serve as electron donors so that the intermediate

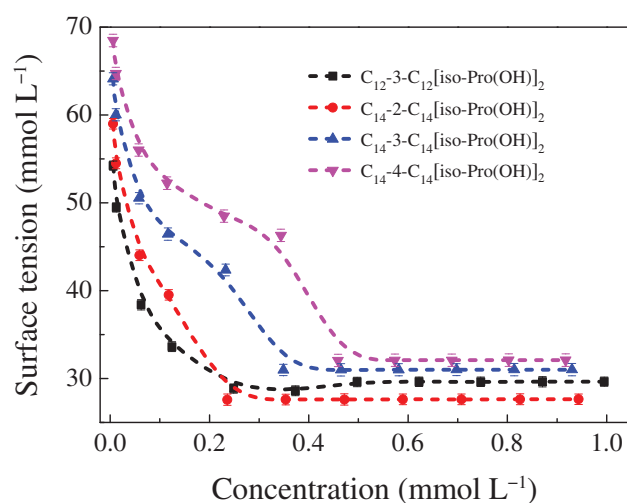


Fig 1 Surface tension *versus* solution concentrations of $C_m\text{-}n\text{-}C_m[\text{iso-Pr}(\text{OH})_2]$ surfactants dispersed in distilled water at 30 °C. Error bar = RSD (n = 3)

products are strong nucleophiles. Furthermore, the reaction center of dibromoalkanes is the carbon atom bound to bromine, which is positively charged due to C-Br being a polar covalent bond. Accordingly, a nucleophilic reaction occurs between the intermediate product and dibromoalkane.

Chemical Structure Characterization

The FT-IR and ^1H NMR spectroscopies of $C_m\text{-}n\text{-}C_m[\text{iso-Pr}(\text{OH})_2]$ surfactants are shown in Fig. S1.

$C_{14}\text{-}2\text{-}C_{14}[\text{iso-Pr}(\text{OH})_2]$: FT-IR (KBr): 3385 cm^{-1} v (–OH), 2906 cm^{-1} , 2857 cm^{-1} s (C–H in –CH₃ or –CH₂–), 1251 cm^{-1} s (C–N), and 724 cm^{-1} v (C–H in (CH₂)_n).

$C_{14}\text{-}2\text{-}C_{14}[\text{iso-Pr}(\text{OH})_2]$: ^1H NMR (CDCl₃, 400 MHz, δ): 0.82 (t, 6H, CH₃–(CH₂)₁₀–, a-H), 1.02 (d, 12H, CH₃–CH(CH₂OH)–, b-H), 1.24 (m, 40H, CH₃–(CH₂)₁₀–, c-H), 1.76 (m, 8H, –CH₂–CH₂–N⁺–CH₂–CH₂–, d-H), 3.19 (t, 8H, –CH₂–N⁺–CH₂–, e-H), 3.42 (d, 8H, –CH(CH₂OH)–N⁺, f-H), 4.32 (m, 8H, CH₃–CH(CH₂OH)–N⁺, g-H), 4.80 (d, 4H, –CH(CH₂OH), h-H).

Water-Air Interface Properties

Fig. 1 shows the change of surface tensions of $C_m\text{-}n\text{-}C_m[\text{iso-Pr}(\text{OH})_2]$ solutions with different concentrations at 30 °C. As can be seen that the surface tension is decreased when the surfactant concentration is increased, indicating the gradual accumulation of the surfactant molecules at the water-air interface with an increase in the surfactant concentration. After a certain concentration, the surface tension remains nearly constant. This concentration is regarded as the critical micellization concentration (CMC). In Table 1, the CMC of $C_{12}\text{-}3\text{-}C_{12}[\text{iso-Pr}(\text{OH})_2]$ is higher than that of

Table 1 Physicochemical properties of C_m - n - C_m [iso-Pr(OH)]₂ surfactants, C₁₂TAB, and C₁₂-3-C₁₂

Surfactants	CMC (mmol L ⁻¹)	γ_{CMC} (mN m ⁻¹)	Π_{CMC} (mN m ⁻¹)	Γ_{max} (mmol m ⁻²)	A_{min} (nm ²)
C ₁₂ -3-C ₁₂ [iso-Pr(OH)] ₂	0.37	28.61	43.34	1.36×10^{-3}	1.22
C ₁₄ -2-C ₁₄ [iso-Pr(OH)] ₂	0.24	27.59	44.36	1.29×10^{-3}	1.29
C ₁₄ -3-C ₁₄ [iso-Pr(OH)] ₂	0.34	30.98	40.97	1.17×10^{-3}	1.42
C ₁₄ -4-C ₁₄ [iso-Pr(OH)] ₂	0.46	32.07	39.88	1.08×10^{-3}	1.54
C ₁₂ TAB (Hao et al., 2019)	14.50	38.00	33.95	3.10×10^{-3}	0.53
C ₁₂ -3-C ₁₂ (Silva et al., 2013)	0.77	34.50	37.45	2.04×10^{-3}	0.81

CMC is the critical micellization concentration, γ_{CMC} is the surface tension at CMC, Π_{CMC} is the effectiveness of surface tension reduction, Γ_{max} is the maximum surface excess, A_{min} is the minimum surface area per molecule.

dodecyltrimethylammonium bromide (C₁₂TAB). Due to the Gemini surfactant structure, the hydrophilicity conferred by the second head group is largely counter balanced by the increased hydrophobicity conferred by the second alkyl tail and the spacer (Pinazo et al., 2019). Consequently, C₁₂-3-C₁₂[iso-Pr(OH)]₂ shows a lower CMC than C₁₂TAB. Besides, it is found that the CMC of C₁₂-3-C₁₂[iso-Pr(OH)]₂ is almost two times higher than that of 1,3-dibromopropane-bis(dodecyl ammonium) dibromide (C₁₂-3-C₁₂). This is due to the hydroxypropyl groups in C₁₂-3-C₁₂[iso-Pr(OH)]₂ structure that facilitates the aggregation of the surfactant molecules in the aqueous solution.

As shown in Table 1, with an increase of the alkyl tail length, the CMC value is decreased, which indicates that the longer the alkyl tail, the stronger the hydrophobic effect between the alkyl tail, thus making it easier to form micelles. The surface tension at CMC (γ_{CMC}) is increased by increasing the alkyl tail length. Because the longer alkyl tail has a higher possibility to rotate and curl freely so that more CH₂ groups are exposed to the interface instead of CH₃ end groups, and CH₂ groups have higher surface energy than CH₃ groups according to Zisman's content of surface energy (Wang et al., 2019). Accordingly, an increase in the γ_{CMC} value is observed when the alkyl tail is lengthened. Furthermore, with the spacer chain length increasing, the CMC is increased. Since the distance between the head groups of the surfactant molecules increases due to the increase of the spacer chain length, which makes it for surfactant molecules more difficult to aggregate in the solution. Lengthening the spacer also lowers the packing efficiency of the surfactant molecules at the water-air interface and thus increases the γ_{CMC} value.

Surface pressure (Π_{CMC}), the effectiveness of the surface tension reduction, is obtained based on Eq. (2) (Jiang et al., 2015).

$$\Pi_{CMC} = \gamma_0 - \gamma_{CMC} \quad (2)$$

where γ_0 is the surface tension of distilled water. γ_{CMC} is the surface tension of the surfactant solution at CMC. As is noticed from the table, compared with C₁₂TAB and C₁₂-

3-C₁₂, whose Π_{CMC} values are 33.95 mN m⁻¹ and 37.45 mN m⁻¹, respectively, Π_{CMC} values of C_m - n - C_m [iso-Pr(OH)]₂ are larger, proving that C_m - n - C_m [iso-Pr(OH)]₂ have superior surface activity than C₁₂TAB and C₁₂-3-C₁₂.

The maximum adsorption capacity (Γ_{max}), the effective measure of the adsorption at the water-air interface, is obtained *via* Eq. (3) (Cheng et al., 2017).

$$\Gamma_{max} = \frac{1}{2.303nRT} \left(\frac{\partial \gamma}{\partial \log C} \right)_T \quad (3)$$

where the value $n = 2$. R is the ideal gas law constant. T is the absolute temperature. $\partial \gamma / \partial \log C$ is the slope of the decreasing part of the surface tension plot below CMC.

Area per molecule (A_{min}) refers to the surface area occupied by one surfactant molecule at the interface, which is calculated *via* Eq. (4) (Cheng et al., 2017).

$$A_{min} = \frac{1}{N_A \Gamma_{max}} \quad (4)$$

where N_A is Avogadro's number.

In Table 1, the Γ_{max} value is decreased with the increase of the alkyl or spacer chain length, which states that the surfactant with the smaller spacer or shorter hydrophobic tail has the higher adsorption efficiency at the water-air interface. In addition, lengthening the spacer chain leads to a decrease in the A_{min} value, because the surfactant molecules adsorbed on the interface are decreased due to the long spacer chain, thereby resulting in the increase of the average area at the interface available for each surfactant molecule. If only the alkyl tail length is increased, a minor increase in the area per molecule is observed.

Effect of Salinity on the Water-Air Interface Properties

The results described above show that the surface activity is higher for C₁₄-2-C₁₄[iso-Pr(OH)]₂ dispersed in distilled water than for other surfactants dispersed in distilled water. The influence of salinity on the surface activity of C₁₄-2-C₁₄[iso-Pr(OH)]₂ will now be described.

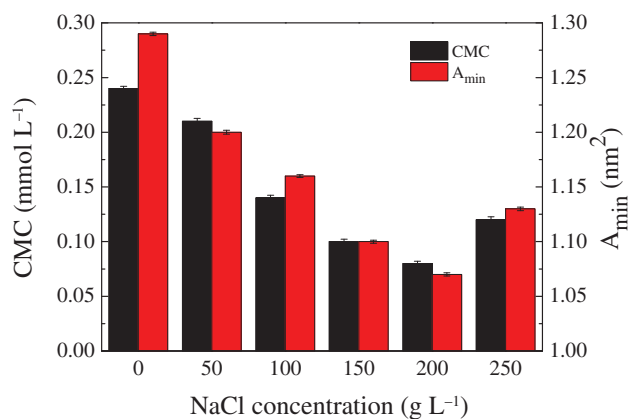


Fig 2 The CMC and A_{\min} values of $C_{14-2-C_{14}}[\text{iso-Pr(OH)}]_2$ dispersed in different NaCl concentrations at 30 °C. Error bar = RSD (n = 3)

As shown in Fig. 2, the CMC is decreased with the increase of NaCl concentration from 50 to 200 g L⁻¹. Because the chloride ions (Cl⁻) from NaCl solution are attracted to the positively charged head groups of $C_{14-2-C_{14}}[\text{iso-Pr(OH)}]_2$, which results in the decrease of the repulsion forces between the surfactant molecules thus allows them to further aggregate. Furthermore, the density of the surfactant molecules adsorbed on the water-air interface decreases due to the decrease of the repulsion forces, increasing the average interfacial area occupied by each surfactant molecule. The CMC value is increased instead when NaCl concentration is greater than 200 g L⁻¹. Since the salting-out effect brings about a decrease in the density of $C_{14-2-C_{14}}[\text{iso-Pr(OH)}]_2$ molecules in the solution, which is not conducive to form micelles. Besides, the salting-out effect also causes A_{\min} to increase to 1.13 nm². From the experiment results, it is concluded that the optimal NaCl concentration is 200 g L⁻¹, and this concentration will be employed in subsequent experiments.

Effect of Temperature on the Water-Air Interface Properties

The temperature is another potential factor, which affects the water-air interface properties. It is clear from the data in Table 2 that the CMC value is decreased when the temperature is increased from 30 to 90 °C. Since the breakdown of the hydrogen bond between water and the surfactant increases the hydrophobicity of the surfactant, promoting the formation of micelles (Tawfik, 2015). Besides, as the temperature increases, the value of A_{\min} is increased. This is due to a rise in temperature that accelerates the thermal motion of the surfactant molecules and forces more surfactant molecules to desorb from the interface and dissolve into the aqueous phase, thereby increasing the available average area for each surfactant molecule at the interface.

The calculation of thermodynamic parameters at different temperatures deepens knowledge of thermodynamic properties. The standard free energy (ΔG_{mic} and ΔG_{ads}), enthalpy (ΔH_{mic} and ΔH_{ads}), and entropy (ΔS_{mic} and ΔS_{ads}) of micellization and adsorption for $C_{14-2-C_{14}}[\text{iso-Pr(OH)}]_2$ surfactant molecules are calculated using Eq. (5)–(10) (Kamboj et al., 2012).

$$\Delta G_{\text{mic}} = nRT \log \text{CMC} \quad (5)$$

$$\Delta G_{\text{ads}} = \Delta G_{\text{mic}} - (0.06\pi_{\text{CMC}}A_{\min}) \quad (6)$$

$$\Delta S_{\text{mic}} = \frac{\Delta G_{\text{mic}}}{\Delta T} \quad (7)$$

$$\Delta S_{\text{ads}} = \frac{\Delta G_{\text{ads}}}{\Delta T} \quad (8)$$

$$\Delta H_{\text{mic}} = \Delta G_{\text{mic}} + T\Delta S_{\text{mic}} \quad (9)$$

$$\Delta H_{\text{ads}} = \Delta G_{\text{ads}} + T\Delta S_{\text{ads}} \quad (10)$$

In Table 2, the negative values of ΔG_{ads} and ΔG_{mic} indicate that the processes of adsorption and micellization are spontaneous. Besides, ΔG_{ads} has higher negativity values than ΔG_{mic} , stating that the surfactant molecules show a stronger preference to adsorb on the water-air interface, which leads to the alkyl tails having more freedom of motion at the interface. The values of ΔH_{mic} and ΔH_{ads} are all negative at 30–90 °C, implying that the processes of adsorption and micellization are exothermic. The values are less negative for ΔS_{mic} than for ΔS_{ads} . This is due to the more tight arrangement compactness of the surfactant molecules participating in the micellization process, which decreases the repulsion in the surfactant-aqueous phase system thus forms more stable micelles (Dai et al., 2017; Tawfik, 2015).

The Water–Oil Interface Properties

The interfacial tensions of surfactants at different concentrations are investigated at 30 °C, the results are illustrated in Fig. 3; For a given surfactant, there is a dramatic decrease in the interfacial tension with increasing surfactant concentration. This is due to the surfactant molecules failing to form tight adsorption layers at the water–oil interface. When the surfactant concentration is further increased, the interfacial tension reaches the minimum value and then tends to stabilize, stating an adsorption saturation for the surfactant molecules at the interface. For a given concentration, the interfacial tensions are lower for $C_m\text{-n-C}_m[\text{iso-Pr(OH)}]_2$ surfactants than for $C_{12}\text{TAB}$ and $C_{12-3-C_{12}}$.

In Fig. 3, the influences of the alkyl tail and spacer chain lengths on the interfacial tension are observed. As can be

Table 2 The values of CMC, A_{\min} , and thermodynamic parameters of $C_{14-2-}C_{14}$ [iso-Pr(OH)]₂ at different temperatures

T (°C)	CMC (mmol L ⁻¹)	A_{\min} (nm ²)	ΔG_{mic} (kJ mol ⁻¹)	ΔG_{ads} (kJ mol ⁻¹)	ΔH_{mic} (kJ mol ⁻¹)	ΔH_{ads} (kJ mol ⁻¹)	ΔS_{mic} (J mol ⁻¹ K ⁻¹)	ΔS_{ads} (J mol ⁻¹ K ⁻¹)
30	0.08	1.05	-19.94	-20.90	-39.89	-41.80	-0.066	-0.069
50	0.06	1.09	-21.86	-23.25	-43.72	-46.50	-0.068	-0.072
70	0.03	1.11	-24.16	-27.44	-48.32	-54.88	-0.071	-0.080
90	0.01	1.14	-28.23	-32.31	-56.47	-64.62	-0.078	-0.089

ΔG_{mic} and ΔG_{ads} refer to the standard free energy of the adsorption and micellization, ΔH_{mic} and ΔH_{ads} refer to the standard enthalpy of the adsorption and micellization, ΔS_{mic} and ΔS_{ads} refer to the standard entropy of the adsorption and micellization.

seen that the interfacial tensions of $C_{12-3-}C_{12}$ [iso-Pr(OH)]₂ and $C_{14-3-}C_{14}$ [iso-Pr(OH)]₂ are very close, implying that the minor effect of the alkyl tail length on the interfacial tension. Besides, the increase of the spacer chain length leads to an increase in the interfacial tension, which indicates that the packing efficiency of the surfactant molecules adsorbed on the water–oil interface is lowered due to increasing the spacer chain length. Therefore, the surfactant molecules with the shorter spacers have a great potential to decrease the interfacial tension.

Foam Properties

Due to its high interfacial energy, foam is thermodynamically unstable. To reduce the interfacial energy and improve foam stability, surfactants are added.

As shown in Fig. 4, for four surfactants (except for C_{12} TAB), with the concentration increasing, the half-life time is increased significantly. This trend occurs because the surfactant molecules can form a tight adsorption layer at the water–air interface due to the increase of the concentration, which makes it difficult for the liquid in foams to

flow from one bubble to another, thereby improving the foam stability. A decrease in the half-life time is observed when the concentration is further increased. Since many micelles are formed in the foam films, the strong electrostatic repulsion existing between the micelles increases the film fragility, and ultimately leads to the decline of foam stability.

It is seen in Fig. 4 that the half time of $C_{12-3-}C_{12}$ [iso-Pr(OH)]₂ is much larger than that of C_{12} TAB. Due to the presence of spacer in $C_{12-3-}C_{12}$ [iso-Pr(OH)]₂ molecules, the interaction between the alkyl tails increases, and the interface film has a certain strength, thereby improving foam stability. When compared with $C_{12-3-}C_{12}$, $C_{12-3-}C_{12}$ [iso-Pr(OH)]₂ has better foam stability. This is due to the mutual attraction of the hydrogen bond formed between hydroxypropyl groups in $C_{12-3-}C_{12}$ [iso-Pr(OH)]₂ molecules that lead to the entanglement between the surfactant molecules, which strengthens the interface film, and finally stabilizes foams. For $C_m-n-}C_m$ [iso-Pr(OH)]₂ surfactants, a slight increase in the half-life time is observed when the alkyl tail is lengthened, indicating the minor effect of the alkyl tail length on foam stability. However, the half-life

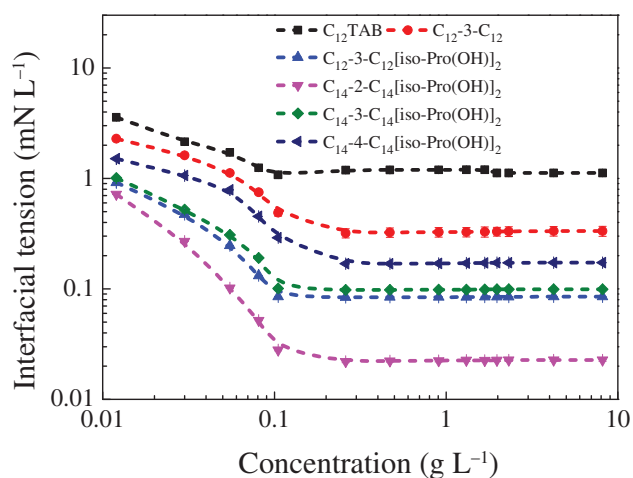


Fig 3 The interfacial tension with different concentrations of $C_m-n-}C_m$ [iso-Pr(OH)]₂, C_{12} TAB and $C_{12-3-}C_{12}$ dispersed in 200 g L⁻¹ NaCl solution at 30 °C. Error bar = RSD (n = 3)

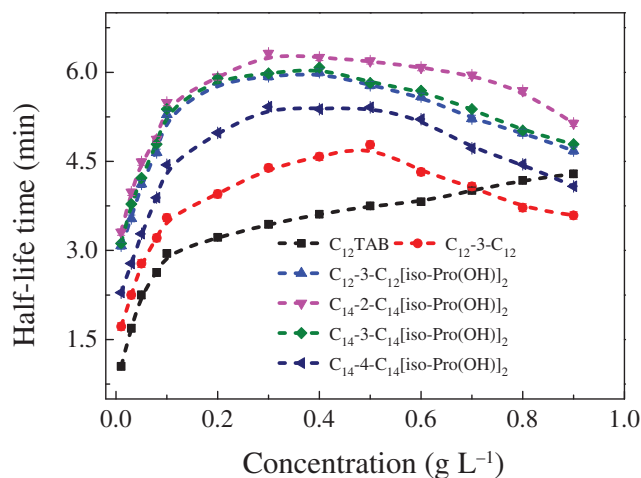


Fig 4 The half-life of foams with different concentrations of $C_m-n-}C_m$ [iso-Pr(OH)]₂, C_{12} TAB and $C_{12-3-}C_{12}$ dispersed in 200 g L⁻¹ NaCl solution at 30 °C. Error bar = RSD (n = 3)

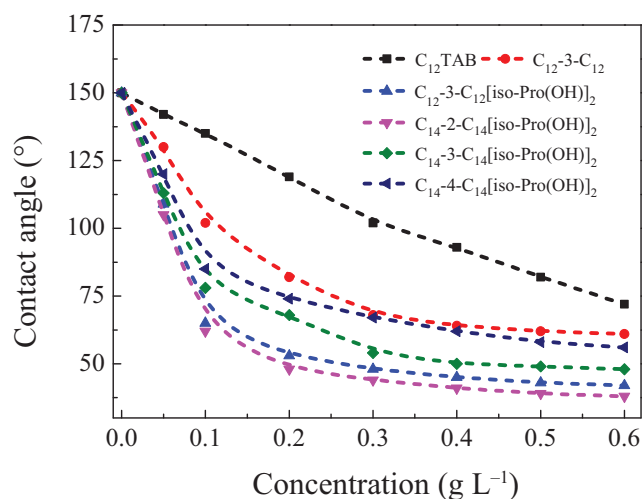


Fig 5 The water contact angle with different concentrations of C_m - n - C_m [iso-Pr(OH)]₂, C_{12} TAB and C_{12} -3- C_{12} dispersed in 200 g L^{-1} NaCl solution at 30°C . Error bar = RSD ($n = 3$)

time is decreased considerably with the spacer chain length increasing. Since the interaction between the alkyl tail is weakened due to lengthening the spacer chain, which is not conducive to enhance the strength of the interfacial film. Consequently, the foam stability becomes worse.

Wettability

Surfactants cause the wettability of rock surface to be changed from originally oil-wet condition to intermediate or even water-wet condition that facilitates spontaneous imbibition of water into the oil-wetted rock, thereby improving oil recovery in low-permeability reservoirs (Kumar and Mandal, 2016). The effect of the surfactant on changing the wettability of the rock surface is evaluated by measuring the water-phase contact angle. Generally, the rock surface is water-wet when the water-phase contact angle ranges from 0° to 75° , intermediate-wet from 75° to 105° , oil-wet from 105° to 180° (Xu et al., 2019).

In Fig. 5, wettability studies are initially performed using NaCl solution (without any surfactant), providing the water-phase contact angle of 148 – 150° , which indicates that the surface of the core is wetted by oil. As the surfactant concentration increases, the water-phase contact angle is decreased remarkably, the variation of water contact angle tends to be slow when the surfactant concentration is greater than CMC. It is observed from Fig. 5 that the lowest water-phase contact angles of the five surfactants are lower than 75° , which states that the core surface altered from oil-wet to water-wet. Since the positively charged head groups of surfactants and carboxylic acid groups in the oil interact to form ion pairs, then the ion pairs are desorbed from the

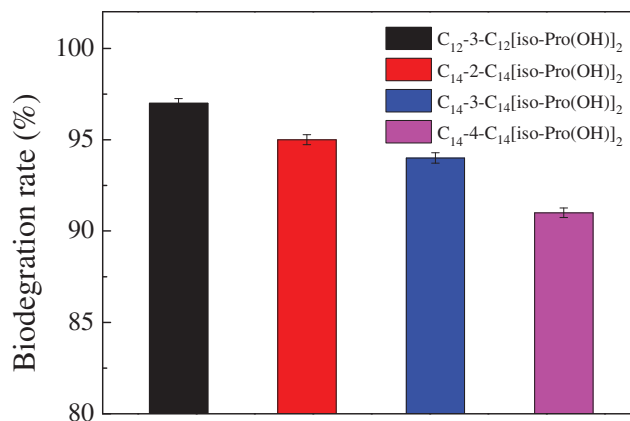


Fig 6 Biodegradation rates of C_m - n - C_m [iso-Pr(OH)]₂ surfactants after 28 days in river water at 30°C . Error bar = RSD ($n = 3$)

core surface and solubilized into micelles. Thus, the core shows a water-wet surface (Hou et al., 2015). The five surfactants can decrease the water-phase contact angle of the oil-wet core to 72° , 61° , 42° , 38° , 48° , and 56° respectively, this difference is explained by Young's equation.

$$\gamma_{s-g} = \gamma_{s-l} + \gamma_{l-g} \cos\theta \quad (11)$$

where θ is the water-phase contact angle. γ_{s-g} , γ_{s-l} , and γ_{l-g} are the interfacial tensions of gas–solid, liquid–solid, and gas–liquid, respectively. While γ_{s-g} and γ_{s-l} are can be regarded as constant due to the internal nature of core and water. C_{14} -2- C_{14} [iso-Pr(OH)]₂ provides the lowest θ value due to its γ_{l-g} value being the lowest, which indicates that C_{14} -2- C_{14} [iso-Pr(OH)]₂ has the best effect of changing the wettability of the oil-wet core among the five surfactants.

Biodegradability

Quaternary ammonium salt surfactants have been employed in many industrial fields. However, it is worth considering whether an increase in surfactant consumption will cause environmental pollution. For this reason, biodegradation has become an important assessment criterion, therefore motivating us to study the biodegradability of C_m - n - C_m [iso-Pr(OH)]₂ surfactants in river water.

The biodegradability of surfactants is enhanced by introducing easily cleavable chemical bonds into the surfactant's structure. Figure 6 shows that C_m - n - C_m [iso-Pr(OH)]₂ surfactants have higher biodegradable rates ($\geq 90\%$ after 28 days) than the biodegradable surfactant of international recommendation (71% after 28 days) at 30°C (Leal et al., 1994). Since C_m - n - C_m [iso-Pr(OH)]₂ surfactants are easy to hydrolyze under alkaline conditions thus have biodegradable and environmental friendly.

Conclusions

Alkanediyl- α,ω -bis[(2-hydroxypropyl)dodecylammonium] dibromide Gemini surfactants (abbreviated as C_m - n - C_m [iso-Pr(OH)]₂ with the alkyl tail length $m = 12, 14$ and the spacer length $n = 2, 3$ and 4) were prepared *via* substitution and quaternization reactions, and their chemical structures have been characterized by FT-IR and ¹HNMR. Besides, the effect of surfactant structure on surface/interfacial activities, foam stability, wettability, and biodegradability were investigated. The results showed that for C_m - n - C_m [iso-Pr(OH)]₂ surfactants, the increase of the alkyl tail length facilitated the formation of micelles. The surface tension was decreased with the spacer length decreasing. The surface activity of C_{14} -2- C_{14} [iso-Pr(OH)]₂ dispersed in 200 g L⁻¹ NaCl solution is higher than that of C_{14} -2- C_{14} [iso-Pr(OH)]₂ dispersed in NaCl solution of other concentrations. Values of thermodynamic parameters calculated from surfactant tension data indicated that the adsorption process was dominated over the micellization process. The water–oil interfacial tension was lower for C_{14} -2- C_{14} [iso-Pr(OH)]₂ than for other surfactants. C_{14} -2- C_{14} [iso-Pr(OH)]₂ solution could generate the most stable foams among other surfactants. The water-phase contact angle reached 38° when the oil-wet core was treated by C_{14} -2- C_{14} [iso-Pr(OH)]₂ solutions with a concentration of 0.6 g L⁻¹. C_m - n - C_m [iso-Pr(OH)]₂ surfactants were highly biodegradable ($\geq 90\%$ after 28 days), which exceeded the international recommendation (71% after 28 days).

Acknowledgements This work was financially supported by the grants from National Natural Science Foundation of China (21376189) and Scientific Research Program of Shaanxi Provincial Education Department (18JC025).

Conflict of Interest The authors declare that they have no conflict of interest.

Reference

- Alami, E., Beinert, G., Marie, P., & Zana, R. (1993) Alkanediyl- α,ω -bis(dimethylalkylammonium bromide) surfactants. 3. Behavior at the air-water interface. *Langmuir*, **9**:1465–1467.
- Bunton, C. A., Robinson, L. B., Schaak, J., & Stam, M. F. (1971) Catalysis of nucleophilic substitutions by micelles of dicationic detergents. *The Journal of Organic Chemistry*, **36**:2346–2350.
- Cheng, Y., Liu, X., Lei, Q., Li, X. F., & Dong, J. F. (2017) Development of novel anionic gemini surfactants and application in fabricating hierarchical silver microparticles for surface-enhanced Raman spectroscopy. *Journal of Colloid and Interface Science*, **505**:1074–1081.
- Dai, C. L., Fang, S. S., Hu, M., He, X. J., Zhao, M. W., Wu, X. P., ... Wu, Y. N. (2017) Synthesis, surface adsorption and micelle formation of a class of morpholinium gemini surfactants. *Journal of Industrial and Engineering Chemistry*, **54**:226–233.
- Hao, J. S., Qin, T., Zhang, Y. B., Li, Y. F., & Zhang, Y. (2019) Synthesis, surface properties and antimicrobial performance of novel Gemini pyridinium surfactants. *Colloids and Surfaces B: Biointerfaces*, **181**:814–821.
- Hegazy, M. A., Rashwan, S. M., Kamel, M. M., & El Kotbb, M. S. (2015) Synthesis, surface properties and inhibition behavior of novel cationic Gemini surfactant for corrosion of carbon steel tubes in acidic solution. *Journal of Molecular Liquids*, **211**:126–134.
- Hou, B. F., Wang, Y. Y., & Huang, Y. (2015) Mechanistic study of wettability alteration of oil-wet sandstone surface using different surfactants. *Applied Surface Science*, **330**:56–64.
- Jiang, Y. J., Geng, T., Li, Q. X., Li, G. J., & Ju, H. B. (2015) Equilibrium and dynamic ST properties of salt-free cationic surfactants with different hydrocarbon chain lengths. *Journal of Molecular Liquids*, **204**:126–131.
- Kamboj, R., Singh, S., Bhadani, A., Kataria, H., & Kaur, G. (2012) Gemini imidazolium surfactants: Synthesis and their biophysicochemical study. *Langmuir*, **28**:11969–11978.
- Kaur, R., Kumar, S., Aswal, V. K., & Mahajan, R. K. (2013) Influence of headgroup on the aggregation and interactional behavior of twin-tailed cationic surfactants with pluronics. *Langmuir*, **29**:11821–11833.
- Kumar, S., & Mandal, A. (2016) Studies on interfacial behavior and wettability change phenomena by ionic and nonionic surfactants in presence of alkalis and salt for enhanced oil recovery. *Applied Surface Science*, **372**:42–51.
- Leal, J. S., Gonzalez, J. J., Kaiser, K. L., Palabrica, V. S., Comelles, F., & Garcia, M. T. (1994) On the toxicity and biodegradation of cationic surfactants. *Acta Hydrochimica et Hydrobiologica*, **22**:13–18.
- Mathias, J. H., Rosen, M. J., & Davenport, L. (2001) Fluorescence study of premicellar aggregation in cationic gemini surfactants. *Langmuir*, **17**:6148–6154.
- Menger, F. M., & Littau, C. A. (1991) Gemini-surfactants: Synthesis and properties. *Journal of the American Chemical Society*, **113**:1451–1452.
- Pinazo, A., Pons, R., Bustelo, M., Manresa, M. Á., Morán, C., Raluy, M., & Pérez, L. (2019) Gemini histidine based surfactants: Characterization; surface properties and biological activity. *Journal of Molecular Liquids*, **289**:111156.
- Sharma, R., Kamal, K., Abdinejad, M., Mahajan, R. K., & Kraatz, H. B. (2017) Advances in the synthesis, molecular architectures and potential applications of gemini surfactants. *Advances in Colloid and Interface Science*, **248**:35–68.
- Silva, S. G., Alves, C., & Cardoso, A. M. S. (2013) Synthesis of gemini surfactants and evaluation of their interfacial and cytotoxic properties: Exploring the multifunctionality of serine as headgroup. *European Journal of Organic Chemistry*, **2013**:1758–1769.
- Tawfik, S. M. (2015) Synthesis, surface, biological activity and mixed micellar phase properties of some biodegradable gemini cationic surfactants containing oxycarbonyl groups in the lipophilic part. *Journal of Industrial and Engineering Chemistry*, **28**:171–183.
- Teresa, G. M., Olga, K., Isabel, R., Brycki, B., Materna, P., & Drgas, M. (2016) Biodegradability and aquatic toxicity of quaternary ammonium-based gemini surfactants: Effect of the spacer on their ecological properties. *Chemosphere*, **154**:155–160.
- Wang, Y. K., Jiang, Y. J., Geng, T., Ju, H. B., & Duan, S. F. (2019) Synthesis, surface/interfacial properties, and biological activity of amide-based Gemini cationic surfactants with hydroxyl in the spacer group. *Colloids and Surfaces A: Physicochemical and Engineering Aspects*, **563**:1–10.
- Wen, Y. Z., Ge, X. J., Gao, W. C., Wei, W. L., Qiao, Y., & Chang, H. H. (2020) Synthesis and aggregation properties of ethylene glycol ester-based cationic Gemini surfactants. *Colloid and Interface Science Communications*, **37**:100274.

- Wu, J. Y., Gao, H. M., Shi, D. D., Yang, Y. F., Zhang, Y. D., & Zhu, W. X. (2020) Cationic gemini surfactants containing both amide and ester groups: Synthesis, surface properties and antibacterial activity. *Journal of Molecular Liquids*, **299**:112248.
- Xu, D. R., Bai, B. J., Wu, H. R., Hou, J. R., Meng, Z. Y., Sun, R. X., ... Kang, W. L. (2019) Mechanisms of imbibition enhanced oil recovery in low permeability reservoirs: Effect of IFT reduction and wettability alteration. *Fuel*, **244**:110–119.